



HAL
open science

Love waves dispersion by phononic pillars for nano-particle mass sensing

Jérémy Bonhomme, Mourad Oudich, Bahram Djafari-Rouhani, Frédéric Sarry,
Yan Pennec, B. Bonello, Denis Beyssen, P. Charette

► **To cite this version:**

Jérémy Bonhomme, Mourad Oudich, Bahram Djafari-Rouhani, Frédéric Sarry, Yan Pennec, et al..
Love waves dispersion by phononic pillars for nano-particle mass sensing. Applied Physics Letters,
2019, 114 (1), pp.013501. 10.1063/1.5068681 . hal-02074727

HAL Id: hal-02074727

<https://hal.science/hal-02074727>

Submitted on 24 May 2022

HAL is a multi-disciplinary open access archive for the deposit and dissemination of scientific research documents, whether they are published or not. The documents may come from teaching and research institutions in France or abroad, or from public or private research centers.

L'archive ouverte pluridisciplinaire **HAL**, est destinée au dépôt et à la diffusion de documents scientifiques de niveau recherche, publiés ou non, émanant des établissements d'enseignement et de recherche français ou étrangers, des laboratoires publics ou privés.

Love waves dispersion by phononic pillars for nano-particle mass sensing

Cite as: Appl. Phys. Lett. **114**, 013501 (2019); <https://doi.org/10.1063/1.5068681>

Submitted: 17 October 2018 • Accepted: 15 December 2018 • Published Online: 03 January 2019

 J. Bonhomme, M. Oudich, B. Djafari-Rouhani, et al.



View Online



Export Citation



CrossMark

ARTICLES YOU MAY BE INTERESTED IN

[Numerical characterization of Love waves dispersion in viscoelastic guiding-layer under viscous fluid](#)

Journal of Applied Physics **128**, 154502 (2020); <https://doi.org/10.1063/5.0022797>

[Propagation of acoustic waves and waveguiding in a two-dimensional locally resonant phononic crystal plate](#)

Applied Physics Letters **97**, 193503 (2010); <https://doi.org/10.1063/1.3513218>

[One-dimensional surface phononic crystal ring resonator and its application in gas sensing](#)

Applied Physics Letters **115**, 041902 (2019); <https://doi.org/10.1063/1.5090592>

Lock-in Amplifiers
up to 600 MHz



Zurich
Instruments



Love waves dispersion by phononic pillars for nano-particle mass sensing

Cite as: Appl. Phys. Lett. **114**, 013501 (2019); doi: [10.1063/1.5068681](https://doi.org/10.1063/1.5068681)

Submitted: 17 October 2018 · Accepted: 15 December 2018 · Published Online: 03 January 2019





View Online



Export Citation



CrossMark

J. Bonhomme,^{1,2,a)}  M. Oudich,^{1,a)} B. Djafari-Rouhani,³ F. Sarry,^{1,2} Y. Pennec,³ B. Bonello,⁴  D. Beyssen,¹ and P. G. Charette²

AFFILIATIONS

¹ Université de Lorraine, CNRS, Institut Jean Lamour, F-54000 Nancy, France

² Laboratoire Nanotechnologies Nanosystèmes (LN2)-CNRS UMI-3463, Université de Sherbrooke, Sherbrooke, Québec J1K 2R1, Canada

³ Institut d'Electronique, de Micro-électronique et de Nanotechnologie (IEMN-UMR CNRS 8520), Université de Lille, Cité Scientifique, 59652 Villeneuve d'Ascq Cedex, France

⁴ Sorbonne Université, UPMC Université Paris 06, INSP UMR CNRS 7588, 4 Place Jussieu, 75005 Paris, France

ABSTRACT

We present a design of a pillared phononic crystal based structure for Love wave manipulation to achieve high mass sensitivity. The structure is made of phononic micro-pillars constructed by stacking tungsten and SiO₂ layers, distributed on a substrate designed for Love wave propagation. The multilayered pillar allows the creation of bandgaps, which leads to the existence of resonant modes where the elastic energy is confined within the SiO₂ free surface layer of the pillar. We study particularly a resonant mode where this layer exhibits torsional mechanical motion which can only be excited by shear horizontal surface waves. We show that Love wave interaction with the torsional mode gives rise to a sharp attenuation in the surface wave transmission spectrum with a high quality factor. We also study the variation of the mass sensitivity of the system by evaluating the resonant mode's frequency shift induced by a mass perturbation using two theoretical approaches: a perturbation theory based approximation and a numerical method. The system presents very promising mass sensitivity which provides an interesting approach to increase the detection performance of Love wave based bio-sensors.

Published under license by AIP Publishing. <https://doi.org/10.1063/1.5068681>

For decades, we have been witnessing an increasing technological development of biosensors for multiple applications: food processing industry, medical field, and also military to prevent biological attacks. A large set of optical and acoustic sensors were proposed with a race for sensitivity improvement to detect a small amount of molecules. Surface plasmon resonance (SPR)¹ merged as a leading technology for monitoring molecular binding events, but it has rapidly reached its limits in sensitivity. Recent progress in micro-fabrication has promoted the development of biosensors based on the concepts of plasmonic metamaterials^{2,3} and optomechanics⁴ which opened the way toward single molecule detection. In parallel, surface acoustic wave (SAW) based detection has been developed where numerous sensing devices were proposed as

cost-effective systems for biomolecule detection in real time.⁵ The molecular binding events on the surface are monitored by measuring the wavelength shift due to the variation of the surface wave velocity mainly caused by the mass loading in the sensing layer. The SAW based devices have the advantage of being miniaturized, embedded in a lab-on-a-chip, and designed in flexible thin substrates and even to be passive sensors with wireless excitation and measurement for remote monitoring.^{6,7} However, the sensitivity of the proposed SAW devices is limited and they are far from competing with recent plasmonic technologies and taking the challenge of detecting a small amount of molecules.

In this letter, we introduce an elastic surface for nano-particle detection with high mass sensitivity. The detection uses phononic crystal (PC) micropillars as resonators where the resonant modes are excited by Love waves. The latter are used for chemical and biological sensing as they are well-known to be

^{a)}Authors to whom correspondence should be addressed: jeremy.bonhomme@univ-lorraine.fr and mourad.oudich@univ-lorraine.fr

very sensitive to mass loading with weak elastic energy loss in liquid environments.^{8,9} PCs are composite materials highly dispersive for elastic waves and can present frequency bandgaps (BGs) where wave propagation is prohibited.^{10,11} They opened the way for multiple acoustic applications such as filtering,^{12,13} sensing,^{14–24} and acoustic wave focusing.^{25,26} They are the starting point for the concept of acoustic metamaterials (AM),²⁷ topological phononics,²⁸ and zero-index elastic/acoustic metamaterials²⁹ which opened numerous possibilities to design sub-wavelength patterned structures for precise acoustic wave manipulations that would have been considered impossible to achieve. Elastic wave control in the ultrasonic regime is of great importance for sensing and optomechanics. Over the last decade, the phononic community highly focused their interest on elastic wave interaction with micro-pillar shaped resonators. The coupling between elastic waves and the resonant modes of individual pillars can be used to produce elastic BG at a sub-wavelength scale^{30–33} or to generate propagating elastic waves by exciting the resonant modes of the pillars.³⁴ Outstanding studies have been conducted for both Rayleigh and Love wave interaction with pillars.^{35–39} The coupling between SAW and the pillar resonant modes occurs below the sound cone which limits the energy leakage into the bulk substrate through SAW-to-bulk wave's conversion. Elastic energy carried by SAW can also be confined or guided within a chain of micro-pillars for instance.⁴⁰ However, there has been no investigation on the performance of the pillar based SAW structure for particle or molecular sensing although many groups in the phononic and AM communities highly believe in their potential for sensing.^{14–24}

In this work, we investigate theoretically the mass sensitivity of the AM based Love SAW (LSAW) structure which typically consists of resonant pillars with a spectrally narrow band response and a high local field concentration. Each pillar is a phononic structure composed of successive tungsten and silica layers, which has the ability to create BG where highly confined resonant modes can be designed for instance at the surface of the pillar or in a cavity inserted in the multilayered pillar.^{41,42} We first introduce a one-dimensional multilayer PC made of successive layers of silica (SiO₂) and tungsten (W) where all the layers have the same thickness $h = 3 \mu\text{m}$ and diameter $d = 6 \mu\text{m}$ [Fig. 1(a)]. Using the finite element (FE) method, we calculated the band structure (BS) along the periodicity, i.e., k_z direction, for the infinite pillar reduced to a unit cell with periodic boundary conditions. The BS shows the existence of three BGs ranging from 167 MHz to 297.5 MHz, from 317 MHz to 360 MHz, and from 368.5 MHz to 388.5 MHz [Fig. 1(b)].

From the infinite PC, we consider a phononic pillar made of five layers with the SiO₂ layer on its both ends [Fig. 2(a)]. We have recently shown that this kind of pillar can give rise to resonant modes where the mechanical vibrations are confined either at the surface of the pillar or in the layers in contact with the substrate.⁴¹ The pillar is deposited on a substrate where LSAW can be generated to interact with the resonant modes. To present the results in the frame of a realistic structure, the substrate is made of a 90°-Z-rotated ST-cut quartz (90STQ)

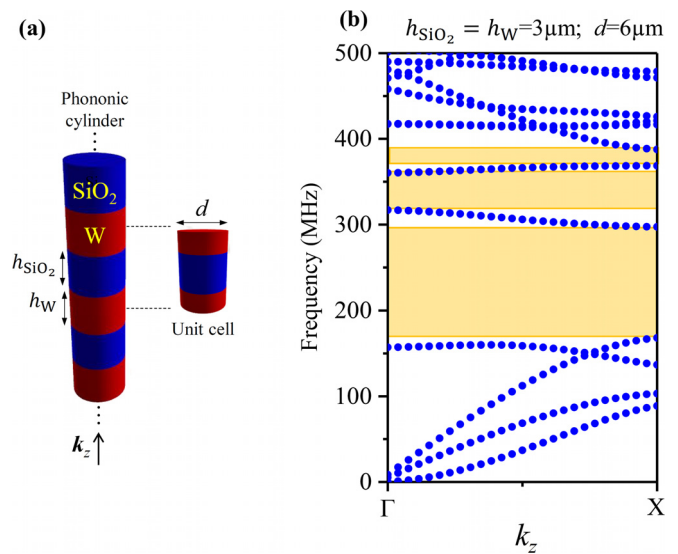


FIG. 1. (a) Phononic pillar made of alternating SiO₂ and W layers. (b) The band structure calculated along the k_z direction for $h = h_W = h_{\text{SiO}_2} = 3 \mu\text{m}$ and $d = 6 \mu\text{m}$.

covered by a silica film with a thickness of $4.2 \mu\text{m}$. We investigate the LSAW interaction with one row of phononic pillars by performing transmission calculations using the model presented in Fig. 2(a). We consider a unit cell along the y axis with periodic conditions to model the infinite repetition of the system. The distance between two adjacent pillars in the y direction is $7 \mu\text{m}$. Except the upper surface which is free, we use perfectly matched layers (PMLs) at the boundaries of the domain modeling the substrate as shown in Fig. 2(a) to avoid the Love and bulk wave reflections. To generate the LSAW, the excitation was performed by applying a voltage on surface boundaries as IDT electrodes between the quartz substrate and the SiO₂ guiding layer [Fig. 2(a)].^{43,44} Based on our recent work,^{41,42} an optimization process was conducted upon the thickness of the bottom SiO₂ layer of the pillar in contact with the substrate. The purpose of this process is to avoid the overlapping of the frequency bands of localized modes where the elastic energy is confined on the bottom and upper layers of the pillar. Figure 2(b) presents the transmission spectra where the SiO₂ and W layers in the pillar have the same thickness ($3 \mu\text{m}$) except for the bottom layer which is chosen to be $1 \mu\text{m}$ thick [Fig. 2(a)]. The transmission curve shows two sharp dips in the amplitude of the total displacement field, which occur at around 244 MHz and 250 MHz where the LSAW attenuation reaches 54% and 90%, respectively. At these two frequencies, we plot in Figs. 2(c) and 2(d) the total displacement field in the phononic pillar as well as the u_y component in the substrate which is the main component of the LSAW. For the sake of clarity, we also represent the displacement field shape (with an appropriate scale factor) for each point of the pillar at the same instant of time chosen for $u_y(\mathbf{x}, t)$ in the substrate. We can clearly deduce that the dips originate from the excitation of resonant modes within the top free SiO₂ layer on the pillar where the mechanical energy is mainly

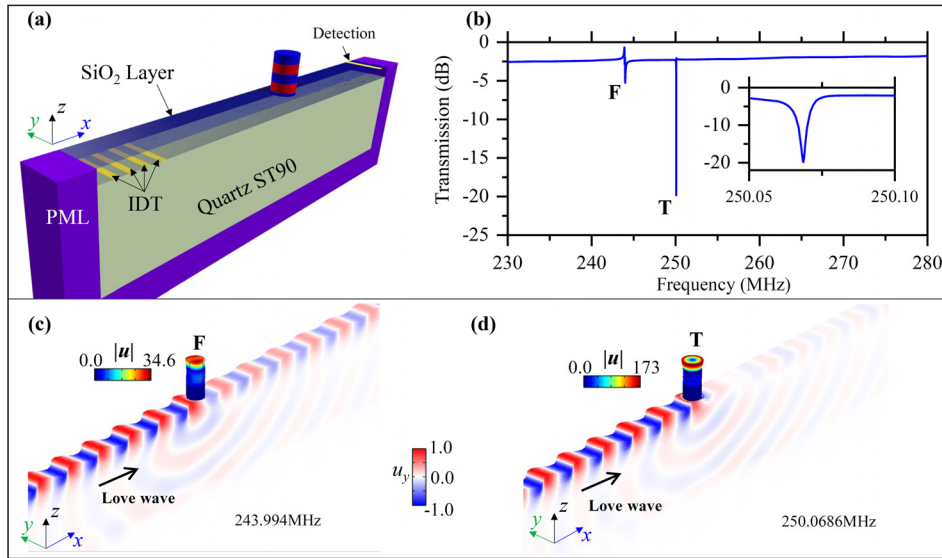


FIG. 2. (a) Schematic representation of the unit cell used for FEM simulation of the system. (b) LSAW transmission result: normalized attenuation of the transmitted signal (in dB); the F and T dips correspond to the flexural and the torsional modes, respectively. The inset shows an enlargement of dip T. Displacement field amplitude for the F (c) and T (d) modes at their resonance frequencies as well as the u_y component in the silica guiding layer.

confined and the maximum of the displacement field amplitude is located. This amplitude quickly decays along the first top SiO_2/W layers in the pillar with almost no vibration in the bottom layers. This behavior can be explained by the presence of the BG which prohibits propagation along the whole pillar. Furthermore, we can observe from Figs. 2(c) and 2(d) that the first mode, denoted F at 244 MHz, displays flexural mechanical vibrations on the free SiO_2 layer in the pillar, while the second mode, denoted T at 250 MHz, has torsional strain. The coupling between the LSAW and the resonant mode T appears to be stronger than the case of mode F as the attenuation is higher for mode T. In fact, when analyzing the mechanical vibration amplitude in the pillar, the maximum of the displacement field amplitude in the pillar is two orders of magnitude higher than the amplitude of LSAW in the case of mode T, while this ratio is only one order of magnitude for the flexural resonant mode F. The two dips experience high mechanical QF which reaches 2250 and 8.3×10^4 for modes F and T, respectively. The torsional resonant mode T presents an interesting mechanical energy confinement with high QF, which could be very promising for sensing application. This confinement is due to the amount of the strain energy carried by the LSAW which is transferred into the top of the pillar. The resonant mode is then excited so that the high mechanical vibration amplitude is depicted in the top layer. One can consider this layer as a phononic cavity where the elastic energy can be stored and scattered back along the pillar into the substrate. This mechanism results in a LSAW dip (transmission loss) in the transmission spectrum in a narrow band corresponding to the localized resonant mode.

In the following, we investigate the mass sensitivity of torsional mode T by introducing a simple theoretical approach. Figure 3(a) illustrates the schematic view of the sensing model where a particle of mass δ_m can be detected when it is attached to the pillar's surface at position r_i from the surrounding

medium. The particle binding on the PC micro-pillar modifies locally its mechanical properties, which results in a frequency shift of the resonant mode due to the contribution of the particle's mass δ_m and the mechanical stiffness. In this study, we suppose that the particle size is very small compared to the pillar's dimensions so that only the mass inertia of the particle is considered upon the resonator. We have used two theoretical methods to evaluate the resonance frequency shift. The first

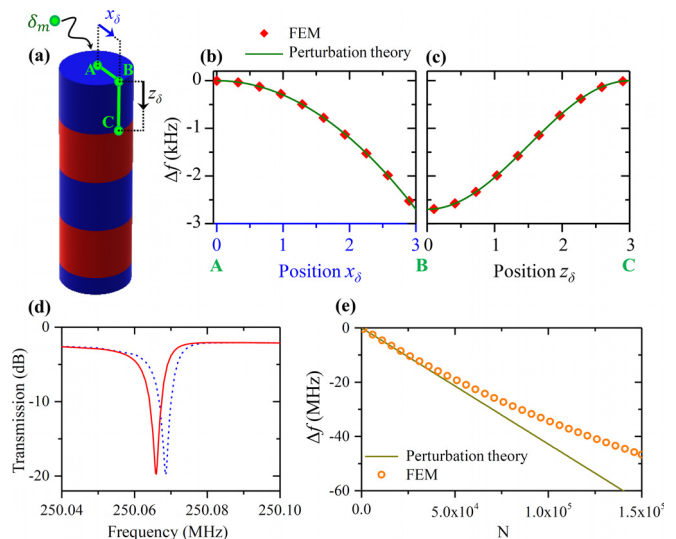


FIG. 3. (a) Schematic representation of the mass perturbation for a punctual mass. (b) and (c) Frequency shift of the torsional mode along the paths [AB] and [BC] in the pillar calculated using the perturbation theory (solid line) and the FEM based numerical method (red diamond scatters). (d) Transmission calculation for the case without (blue dashed line) and with mass perturbation (red solid line). (e) Frequency shift of mode T as a function of the particle number N. Comparison between the perturbation theory and numerical simulations.

one is a semi-analytical formula based on the perturbation theory.^{45,46} The fractional frequency shift for a small size particle (less than 100 nm such as a virus) positioned at r_i is given by the following formula:

$$\frac{\delta\omega}{\omega_0} = -\delta_m \frac{\|\mathbf{u}(r_i)\|^2}{2 \int_V \rho \|\mathbf{u}\|^2 dv}, \quad (1)$$

where ω is the angular frequency, \mathbf{u} is the displacement field, and the integral in the denominator is taken over the whole volume of the resonator which contains the overwhelming majority of the elastic energy.

Meanwhile, for a large amount of molecules distributed over the pillar's surface over random locations, we account for them by summing the single contribution (1) over a number of N randomly located molecules and turn the discrete sum into integral over the surface

$$\frac{\delta\omega}{\omega_0} = -\delta_m \sigma \frac{\int_S \|\mathbf{u}\|^2 ds}{2 \int_V \rho \|\mathbf{u}\|^2 dv}, \quad (2)$$

where $\sigma = N/S$ is the molecule surface density. The displacement fields in formulas (1) and (2) are for the unperturbed state, and they are calculated numerically using the eigenfrequency solver in Comsol Multiphysics[®] for the torsional mode.

The second method considered for the mass sensitivity estimation is numerical where the mass effect for a single molecule is evaluated by introducing the following point force:⁴⁷

$$\mathbf{F}_i = \delta_m \omega^2 \mathbf{u}(r_i). \quad (3)$$

For N molecules distributed on the surface of the pillar, a force per unit area is applied using the expression

$$\mathbf{F}_s = \delta_m \sigma \omega^2 \mathbf{u}. \quad (4)$$

In this study, the particle is considered as a rigid mass and we neglect the effect of its stiffness on the pillar as its size is way smaller than the dimensions of the pillar and the strain associated with the torsional mode. The mass was added in the model by using the weak contribution option in Comsol.

For the calculation, we consider for instance a typical mass of a virus cell $\delta_m = 1.15fg$ (approximate mass of an HIV-1 virus⁴⁸) attached on a point r_i and we looked for the eigenfrequencies of the localized torsional mode. By taking into account the symmetry of this mode upon the displacement field and strain [see Fig. 2(d)], we can study the mass effect for positions r_i at the surface of the top free layer of the pillar along the radial path indicated by [AB] in Fig. 3(a) and along a line in the lateral curved surface indicated by path [BC] in the same figure. Figures 3(b) and 3(c) display the T mode's frequency shift caused by the mass δ_m as a function of its positions x_s and z_s described in Fig. 3(a) along paths [AB] and [BC], respectively. The green solid curve and the red diamond scatters are the results given by the first order perturbation theory formula (1) and FEM [expression (3)], respectively. One can clearly see from Fig. 3(b) that the frequency shift is almost zero at

point A and decreases to reach its maximum absolute value of 2.7 kHz at point B. The negative sign indicates that the mode's frequency shifts down to lower frequencies. This can be expected when looking closely into the mechanical motion of the torsional mode where the displacement field is zero at the center and maximum in the circumference of the SiO₂ cylindrical layer. In Fig. 3(c), the frequency shift becomes zero at the interface between the top SiO₂ layer and the W layer (point C), which is expected since the elastic energy is confined within the top SiO₂ layer of the phononic pillar. We can also clearly deduce that the semi-analytical formula (1) and the FEM model give the same results. Besides, we plot in Fig. 3(d) the LSAW transmission through a row of pillars where the blue curve presents the resonance dip caused by the T mode without the mass and the red curve the transmission for the case where the mass δ_m is attached to the pillar at point B where the maximum frequency shift is expected. We can clearly see the shift of the mode's dip into lower frequencies by almost 2.7 kHz which corresponds to the shift result predicted from the eigenfrequency calculation.

Meanwhile, for the case of an amount of N particles distributed homogeneously in the pillar's entire surface, Fig. 3(e) displays the frequency shift of the T mode as a function of the particle number N using the perturbation theory and the numerical method presented by the solid line and circles, respectively. Both methods give the same frequency shift result up to 3×10^4 particles where it reaches approximately -15 MHz, and then, the two results become significantly different. The linear formula (2) derived from the first order perturbation theory becomes no longer valid for N higher than 3×10^4 so that higher orders must be considered to fit the numerical curve.

The phononic crystal pillar undergoes interesting mechanical behavior which can be used for elastic wave manipulation. The phononic BG allows the existence of resonant modes localized within the top layer of the pillar which can be efficiently excited by LSAW. The elastic coupling can be depicted in the LSAW transmission spectrum as a narrow band sharp decay. Particularly, the LSAW can be used to excite a torsional mode in the pillar depicted in the transmission spectrum as a dip with high QF. This mode presents an interesting mass sensitivity for single-particle detection which is evaluated by two theoretical approaches: a perturbation theory based approximation and a FEM based numerical method. From a practical point of view, the pillar surfaces can be functionalized to be able to capture the targeted molecule (virus, DNA, protein ...). The surface chemistry allows adding bioreceptors on the top and sides of the cylinder where the molecule can be attached. The effect of the chemical layer on the bioreceptors is not considered in this study. But it should have the same effect as a uniform repartition of mass along the cylinder, and so, it will shift the resonant frequency. The system pillar and bioreceptor layer become the unperturbed system. The molecular binding event can be monitored through a real time observation of the mechanical frequency shift of the PC resonant modes in the LSAW spectrum. This mechanical system can be used to introduce a future sensing approach using PC in LSAW based devices to increase the performance of nano-particle and bio-molecule sensing.

The authors would like to thank the CNES (Centre National d'Etudes Spatiales) and the CNRS (Centre National de la Recherche Scientifique) for financial support.

The author M.O. would like to thank Wafae Fella Mihoubi and Hugo Freyermuth for their involvement in this work.

REFERENCES

- ¹J. N. Anker, W. P. Hall, O. Lyandres, N. C. Shah, J. Zhao, and R. P. Van Duyne, *Nat. Mater.* **7**, 442 (2008).
- ²C. Wu, A. B. Khanikaev, R. Adato, N. Arju, A. Ali Yanik, H. Altug, and G. Shvets, *Nat. Mater.* **11**, 69 (2012).
- ³K. V. Sreekanth, Y. Alapan, M. ElKabbash, E. Ilker, M. Hinczewski, U. A. Gurkan, A. De Luca, and G. Strangi, *Nat. Mater.* **15**, 621 (2016).
- ⁴W. Yu, W. C. Jiang, Q. Lin, and T. Lu, *Nat. Commun.* **7**, 12311 (2016).
- ⁵K. Länge, B. E. Rapp, and M. Rapp, *Anal. Bioanal. Chem.* **391**, 1509 (2008).
- ⁶C. Lim, W. Wang, S. Yang, and K. Lee, *Sens. Actuators B* **154**, 9 (2011).
- ⁷H. Jin, J. Zhou, X. He, W. Wang, H. Guo, S. Dong, D. Wang, Y. Xu, J. Geng, J. K. Luo, and W. I. Milne, *Sci. Rep.* **3**, 2140 (2013).
- ⁸J. Du, G. L. Harding, J. A. Ogiwly, P. R. Dencher, and M. Lake, *Sens. Actuators Phys.* **56**, 211–219 (1996).
- ⁹P. Tang, Y. Wang, J. Huo, and X. Lin, *Polymers* **10**, 563 (2018).
- ¹⁰M. S. Kushwaha, P. Halevi, L. Dobrzynski, and B. Djafari-Rouhani, *Phys. Rev. Lett.* **71**, 2022–2025 (1993).
- ¹¹M. S. Kushwaha, P. Halevi, G. Martínez, L. Dobrzynski, and B. Djafari-Rouhani, *Phys. Rev. B* **49**, 2313–2322 (1994).
- ¹²Y. Pennec, B. Djafari-Rouhani, J. O. Vasseur, A. Khelif, and P. A. Deymier, *Phys. Rev. E* **69**, 046608 (2004).
- ¹³C. Qiu, Z. Liu, J. Mei, and J. Shi, *Appl. Phys. Lett.* **87**, 104101 (2005).
- ¹⁴R. Lucklum and J. Li, *Meas. Sci. Technol.* **20**, 124014 (2009).
- ¹⁵M. Zubtsov, R. Lucklum, M. Ke, A. Oseev, R. Grundmann, B. Henning, and U. Hempel, *Sens. Actuators, A* **186**, 118 (2012).
- ¹⁶A. Sato, Y. Pennec, T. Yanagishita, H. Masuda, W. Knoll, B. Djafari-Rouhani, and G. Fytas, *New J. Phys.* **14**, 113032 (2012).
- ¹⁷R. Lucklum, M. Ke, and M. Zubtsov, *Sens. Actuators, B* **171–172**, 271 (2012).
- ¹⁸A. Oseev, R. Lucklum, and M. Zubtsov, *Sens. Actuators, B* **189**, 208 (2013).
- ¹⁹A. Salman, O. A. Kaya, and A. Cicek, *Sens. Actuators, A* **208**, 50 (2014).
- ²⁰A. Salman, O. A. Kaya, A. Cicek, and B. Ulug, *J. Phys. D: Appl. Phys.* **48**, 255301 (2015).
- ²¹S. Amoudache, Y. Pennec, B. Djafari-Rouhani, A. Khater, R. Lucklum, and R. Tigrine, *J. Appl. Phys.* **115**, 134503 (2014).
- ²²S. Amoudache, R. Moiseyenko, Y. Pennec, B. Djafari-Rouhani, A. Khater, R. Lucklum, and R. Tigrine, *J. Appl. Phys.* **119**, 114502 (2016).
- ²³R. Lucklum and F. Lucklum, *J. Acoust. Soc. Am.* **141**, 3793 (2017).
- ²⁴D. Nardi, E. Zagato, G. Ferrini, C. Giannetti, and F. Banfi, *Appl. Phys. Lett.* **100**, 253106 (2012).
- ²⁵T.-T. Wu, Y.-T. Chen, J.-H. Sun, S.-C. Steven Lin, and T. J. Huang, *Appl. Phys. Lett.* **98**, 171911 (2011).
- ²⁶J. Zhao, B. Bonello, L. Becerra, O. Boyko, and R. Marchal, *Appl. Phys. Lett.* **108**, 221905 (2016).
- ²⁷Z. Liu, X. Zhang, Y. Mao, Y. Y. Zhu, Z. Yang, C. T. Chan, and P. Sheng, *Science* **289**, 1734 (2000).
- ²⁸Z. Yang, F. Gao, X. Shi, X. Lin, Z. Gao, Y. Chong, and B. Zhang, *Phys. Rev. Lett.* **114**, 114301 (2015).
- ²⁹H. Zhu and F. Semperlotti, *Phys. Rev. Appl.* **8**, 064031 (2017).
- ³⁰Y. Pennec, B. Djafari Rouhani, H. Larabi, A. Akjouj, J. N. Gillet, J. O. Vasseur, and G. Thabet, *Phys. Rev. B* **80**, 144302 (2009).
- ³¹Y. Pennec, B. Djafari-Rouhani, H. Larabi, J. O. Vasseur, and A. C. Hladky-Hennion, *Phys. Rev. B* **78**, 104105 (2008).
- ³²T.-T. Wu, Z.-G. Huang, T.-C. Tsai, and T.-C. Wu, *Appl. Phys. Lett.* **93**, 111902 (2008).
- ³³T.-C. Wu, T.-T. Wu, and J.-C. Hsu, *Phys. Rev. B* **79**, 104306 (2009).
- ³⁴Y. Jin, B. Bonello, R. P. Moiseyenko, Y. Pennec, O. Boyko, and B. Djafari-Rouhani, *Phys. Rev. B* **96**, 104311 (2017).
- ³⁵A. Khelif, Y. Achaoui, S. Benchabane, V. Laude, and B. Aoubiza, *Phys. Rev. B* **81**, 214303 (2010).
- ³⁶J. F. Robillard, A. Devos, and I. Roch-Jeune, *Phys. Rev. B* **76**, 092301 (2007).
- ³⁷Y. Achaoui, A. Khelif, S. Benchabane, L. Robert, and V. Laude, *Phys. Rev. B* **83**, 104201 (2011).
- ³⁸D. Yudistira, A. Boes, B. Graczykowski, F. Alzina, L. Y. Yeo, C. M. Sotomayor Torres, and A. Mitchell, *Phys. Rev. B* **94**, 094304 (2016).
- ³⁹T.-T. Wu, C.-S. Liu, and T.-W. Liu, in *IEEE Joint UFFC, EFTF PFM Symposium* (2013), p. 2133.
- ⁴⁰S. Benchabane, R. Salut, O. Gaiffe, V. Soumann, M. Addouche, V. Laude, and A. Khelif, *Phys. Rev. Appl.* **8**, 034016 (2017).
- ⁴¹M. Oudich, B. Djafari-Rouhani, B. Bonello, Y. Pennec, and F. Sarry, *Crystals* **7**, 372 (2017).
- ⁴²M. Oudich, B. Djafari-Rouhani, B. Bonello, Y. Pennec, S. Hemaidia, F. Sarry, and D. Beyssen, *Phys. Rev. Appl.* **9**, 034013 (2018).
- ⁴³T.-W. Liu, Y.-C. Tsai, Y.-C. Lin, T. Ono, S. Tanaka, and T.-T. Wu, *AIP Adv.* **4**, 124201 (2014).
- ⁴⁴T.-W. Liu, Y.-C. Lin, Y.-C. Tsai, T. Ono, S. Tanaka, and T.-T. Wu, *Appl. Phys. Lett.* **104**, 181905 (2014).
- ⁴⁵B. A. Auld, *Acoustic Fields and Waves in Solids* (1990), Vol. 2.
- ⁴⁶R. B. Topolevsky and M. Redwood, *IEEE Trans. Sonics Ultrason.* **22**, 152 (1975).
- ⁴⁷M. Oudich, X. Zhou, and M. B. Assouar, *J. Appl. Phys.* **116**, 193509 (2014).
- ⁴⁸P. Zhu, E. Chertovat, J. Bess, Jr., J. D. Lifson, L. O. Arthur, J. Liu, K. A. Taylor, and K. H. Roux, *Proc. Natl. Acad. Sci. U. S. A.* **100**, 15812 (2003).